SHOCK COMPRESSION OF CONDENSED MATTER - 1989

Proceedings of the American Physical Society Topical Conference held in Albuquerque, New Mexico, August 14–17, 1989

Edited by

S. C. SCHMIDT

Los Alamos National Laboratory
Los Alamos, New Mexico, USA

J. N. JOHNSON

Los Alamos National Laboratory
Los Alamos, New Mexico, USA

L. W. DAVISON

Sandia National Laboratories
Albuquerque, New Mexico, USA

1990

NORTH-HOLLAND
AMSTERDAM • OXFORD • NEW YORK • TOKYO

SHOCK COMPRESSION OF CONDENSED MATTER - 1989
S.C. SCHMIDT, J.N. JOHNSON, L.W. DAVISON (editors)

STRESS-WAVE INDUCED FRAGMENTATION IN ALUMINA-BASED CERAMICS

L. H. LEME LOURO* and M. A. MEYERS**

*Instituto Militar de Engenharia, Urca, Rio de Janeiro, Brazil
**University of California, San Diego, Department of Applied Mechanics and Engineering Sciences, R-011, La Jolla, California, 92093-0411, United States of America

In a series of impact experiments in which the compressive stress, stress duration, and tensile reflection following compression were varied, the effect of these parameters on fragmentation of alumina were quantitatively established. Initiation sites for damage were identified by transmission electron microscopy. A model for fragmentation is developed, based on nucleation, growth, and coalescence of cracks. This model leads to quantitative predictions of damage through the parameter S_V (surface area per unit volume) that is a function of stress-wave and material parameters.

1. INTRODUCTION

Sapphire (monocrystalline alumina) exhibits Hugoniot Elastic Limit (HEL) values up to 21 GPa[1]. Polycrystalline alumina also has a high HEL; it is approximately 10 GPa[2]. Thus, the stress-wave response of alumina, at stress levels on the order of the HEL, is of considerable fundamental and applied importance. The recent studies by Yaziv[3] and Leme Louro[4] provide comprehensive reviews on the subject. A question of great importance is: is there damage under compression at stress levels below the HEL? As a corollary to this question, can one predict quantitatively impact damage in ceramics?

2. EXPERIMENTAL PROCEDURE

The experiments were conducted in a one-stage gas gun at velocities between 200 and 1,000 m/s. The specimens (disk-shaped, with dimensions shown in Fig. 1) were encapsulated in either aluminum or copper containers. Aluminum and copper have shock impedances that are lower and slightly higher than alumina, respectively. Thus, aluminum and copper capsules are expected to generate compression + tension and compression in the alumina disks, respectively. SWAP-7 computations were performed, confirming these stress sequences. Projectiles were of the same material as capsules, as well as the momentum traps. Matching of surfaces between alumina and capsule was very carefully conducted, with individual matching of pairs, in order to decrease, to the extent possible, existing gaps. After impact, the capsules were sectioned and the capsule-alumina sets were impregnated with a dark resin in a vacuum oven in order to more clearly delineate cracks. Crack observation was conducted at three levels: macro, meso, and microscopic. Only macroscopic measurements, based on the linear intercept method, are reported here.

3. EXPERIMENTAL RESULTS

The most significant results are shown in Figures 2, 3, and 4. These results indicate that:

a) Both compressive and tensile stresses generate cracks.

b) S_V (surface area per unit volume) increases with stress (Fig. 2), stress duration (Fig. 3), and is higher for compression + tension than for compression (Fig. 2).

c) The isolated point in Fig. 4 (◪) provides an important insight into the process of fragmentation. In this experiment the back of specimen (marked A in Fig. 1) was filled with epoxy, a low impedance material. This epoxy resulted in an enhancement of the tensile stress, for a same

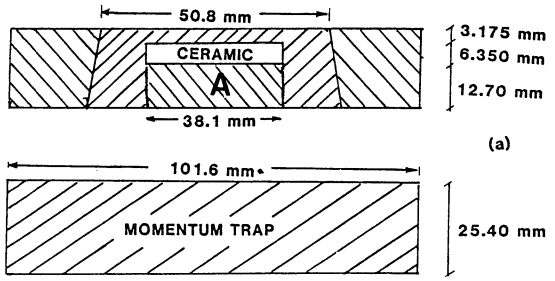

FIGURE 1
Schematic representation showing capsule design.

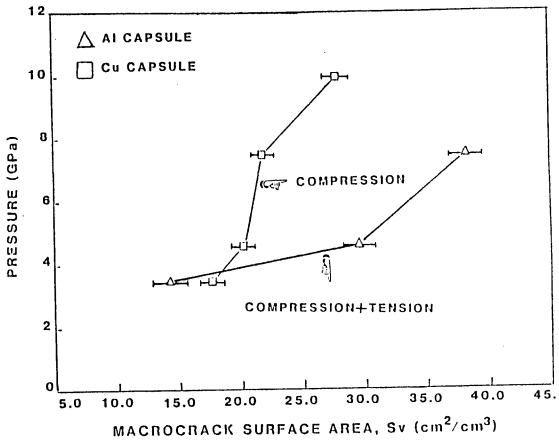

FIGURE 2
Effect of pressure on fragmentation of alumina.

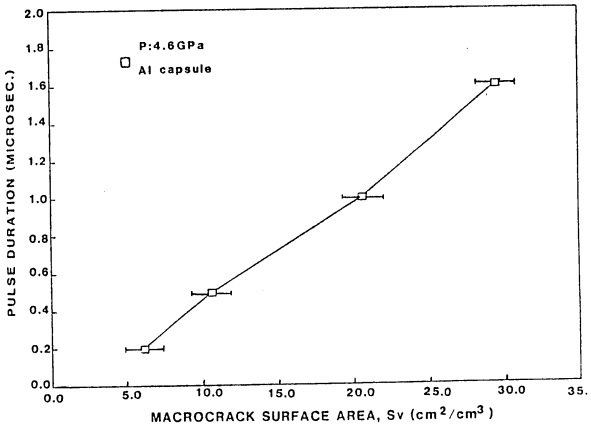

FIGURE 3
Effect of pulse duration on fragmentation of alumina (4.6 GPa compressive stress, aluminum capsule).

level of compressive stress (see Table in Fig. 4). S_V was not proportionately increased; one would expect that this data point would fall on the line that the other points define, in Fig. 4, if fragmentation was purely a tensile phenomenon. One concludes from the above that compressive stresses precondition the material, by creating flaws that can grow under tension.

4. ANALYSIS

A detailed analysis will be presented elsewhere[5]. The main components of the formulation are given here. The upper limit for crack velocity is the Rayleigh wave speed, which is approached asymptotically as the stress intensity

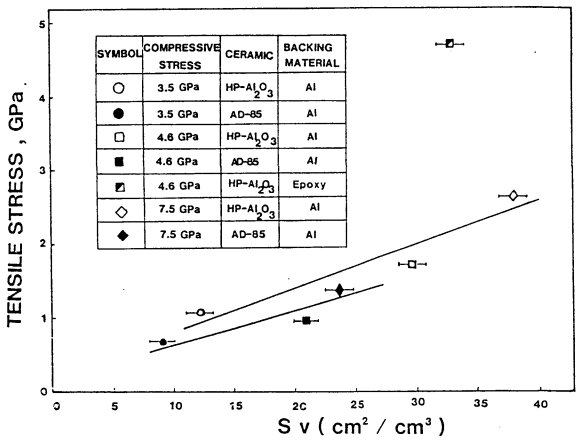

FIGURE 4
Effect of tensile stress on alumina fragmentation.

factor increases. An equation that represents well this behavior is:

$$v_c = v_r\left[1 - e^{\alpha\left(K_I^2 - K_{Ic}^2\right)}\right] \quad (1)$$

where v_c is the crack velocity, v_r the Rayleigh velocity, K_{Ic} the static fracture toughness, K_I the fracture toughness at a velocity v_c, and α a material parameter.

It was possible to obtain the parameter α and therefore describe the dynamic crack propagation response for alumina. The static fracture toughness was taken as 4 MPa $\cdot m^{1/2}$ for high-purity alumina. Suresh[6] measured the fracture toughness of alumina at a crack propagation velocity of approximately 1.2 Km/s and found a value of the order of 1.5 K_{Ic}, that corresponds to 6 MPa $\cdot m^{1/2}$. Thus, the following equation describes the dynamics of crack propagation in alumina:

$$v_c = 5.64\left[1 - e^{-1.2x10^{-2}\left(K_I^2 - 16\right)}\right] \quad (2)$$

The model proposed herein is based on the ideas of crack nucleation, growth, and coalescence developed by the SRI-International group.[7,8] It is assumed that the material has pre-existent flaws (voids, cracks, etc.) which are shown schematically in Fig. 5(a). Under compression, some of these flaws are activated (a stress and time-dependent mechanism). When tension is subsequently applied, growth of the initial cracks takes place at the velocity dictated by Eq. 2, while subcritical flaws are activated in a time-dependent mode. The initial population of flaws is N_i.

When the compressive pulse passes, the pre-existent defects are enlarged and new defects are created. Therefore, the population of flaws changes from N_i to $N_i + N_v'$ as illustrated schematically in Figure 5(a) and (b). N_i is considered the number of pre-existing flaws per unit volume, and N_v' represents the additional number of flaws appearing as a result of the passage of the compressive stress pulse. Hence, N_v' will be a direct function of σ_c (compressive stress level) and t (time of pulse duration). One assumes:

$$N_v = N_i + t\,\sigma_c \cdot \dot{N}_v' \tag{3}$$

$\dot{N}_v'$ is the nucleation rate of flaws under compression.

As illustrated in Figure 5 (c), the crack population is divided into two groups, immediately after the transit of the compressive pulse. The first group contains cracks having at least the critical size or bigger, and the second one involves all cracks smaller than a_c. Beyond a_c the cracks grow with velocity v_c. Below a_c slower subcritical crack growth takes place, and these subcritical cracks may become critical within the time of pulse duration.

Then, one can write that:

$$N_v = N_v^c + N_v^{sc} \tag{4}$$

where N_v^c and N_v^{sc} are the number of flaws with critical and subcritical size per unit volume, respectively. Figure 5(d) represents schematically crack intersections which give rise to fragmentation. Figure 6 illustrates the formation of unloaded regions. The model incorporates the concept of unloaded fraction, since the available volume for crack nucleation and growth decreases as the time increases. The unloaded volume, V_u, can be obtained if one considers the pre-existent critical cracks, each one generating a small unloaded volume V_u', as well as the critical cracks nucleated during the time of stress pulse application. So,

$$V_u = N_v^c\, V_0\, V_u' + \int_0^t V_u' \left(V_0 - V_u\right) dN_v^{sc} \tag{5}$$

where V_0 is the total volume considered. Therefore, the unloaded fraction, f_u, is obtained as:

$$1 - f_u = \exp\left[At + B\right]$$

where,

$$A = -\,V_u'\,\dot{N}_v^{sc} \text{ and } B = \ln\left(1 - N_v^c\, V_u'\right)$$

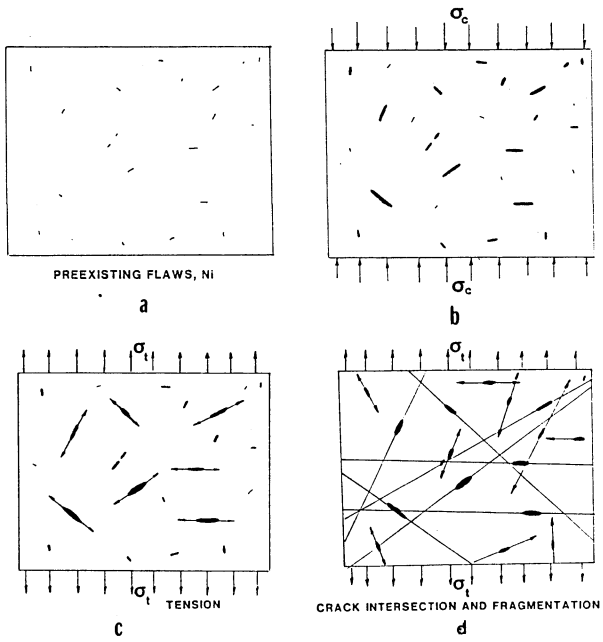

FIGURE 5
Schematic representation showing: (a) ceramic "as-received" with inherent flaws; (b) flaw increase due to compression; (c) critical and subcritical flaws under tension; (d) crack intersection resulting in fragmentation.

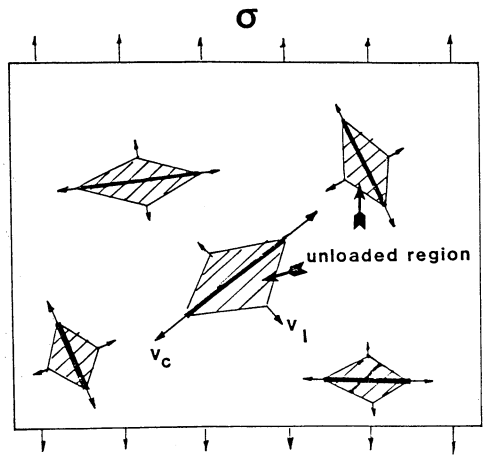

FIGURE 6
Kinetics of fragmentation and unloaded volume surrounding cracks (schematic).

The increase in crack surface with time can be expressed as:

$$dS = \frac{4\pi v_r}{B'^2}\left[\frac{\ln\left(A' + Ce^{v_r t}\right)}{A' + Ce^{v_r t}}\, e^{v_r t}\right] dt \tag{6}$$

where

$$e^{\alpha\sigma_t' \pi a_c} = A'$$
$$\alpha\sigma_t^2\pi = B'$$

$$\frac{e^{1.1B'a_c} - A'}{e^{v_r t_0}} = C$$

The total surface area per unit volume is determined from the progression of cracking with time. Referring to Figure 5, one can calculate the fragmentation as a function of time by considering the following components:

a) Cracks that are critical at the onset of tension (t = 0):

$$S_{v_1} = S_v N_v^c$$

$$S_{v_1} = \frac{2K_{IC}^4}{\sigma_t^4}\left[\left(N_i + t\sigma_t \dot{N}_v'\right) - N_v^{sc}\right] \tag{7}$$

b) Increase in surface area of cracks that are critical at time 0 and that continue to grow. This is equal to the cracks per unit volume, N_v^c, multiplied by the growth rate of these cracks for an interval time $0 \rightarrow t$.

$$S_{V_2} = \frac{4\pi V_r N_V^c e^B}{B'^2} \cdot \frac{1}{C^{1+(A/V_r)_{V_r}}}\left\{(y-A')^{A/V_r}\cdot\frac{1}{2}(\ln y)^2 + \frac{A}{2v_r}\cdot A'^{-1}\left\{y(\ln y)^2 - 2y\ln y + 2y + \frac{1}{A'}\left[\frac{1}{2}y^2 \times (\ln y)^2 - \frac{1}{2}y^2\ln y + \frac{1}{4}y^2\right] + \frac{1}{A'^2}\left[\frac{1}{3}y^3(\ln y)^2 - \frac{2}{9}y^3\ln y + \frac{2}{27}y^3\right]\right\}\right|_{A'+C}^{A'+Cx} \tag{8}$$

where $y = A' + Ce^{v_r t}$

c) The third component of the surface area per unit volume are the cracks that become critical during the interval $0 \rightarrow t$. A nucleation rate $\dot{N}_v^{SC}$ of critical cracks is defined and assumed to be constant. It is assumed that no nucleation takes place in unloaded material.

$$S_{V_3} = \frac{2K^4}{\sigma_t^4}\left[\frac{\left(1 - N_V^C V_u'\right)\left(e^{N_V{}^{SC}} - 1\right)}{V_u'^2\, e^{N_V{}^{SC}}}\right] \tag{9}$$

d) The fourth component of fragmentation is provided by the growth of cracks that become critical during the interval $0 \rightarrow t$. This involves growth of different cracks for different length of time, since each critical crack has a specific nucleation time.

$$S_{V_4} = \frac{4\pi V_r \dot{N}_V^{sc} e^{2B}}{B'^2} \cdot \frac{1}{C^{1+(2A/V_r)_{V_r}}}\left\{(y-A')^{2A/V_r}\cdot\frac{1}{2}(\ln y)^2 + \frac{A}{V_r}\cdot A'^{-1}\left\{y(\ln y)^2 - 2y\ln y + 2y\right] + \frac{1}{A'}\left[\frac{1}{2}y^2 + (\ln y)^2 - \frac{1}{2}y^2\ln y + \frac{1}{4}y^2\right] + \frac{1}{A'^2}\left[\frac{1}{3}y^3(\ln y)^2 - \frac{2}{9}y^3\ln y + \frac{2}{27}y^3\right] + \cdot\right\}\right|_{A'+C}^{A'+Cx} \tag{10}$$

The nucleation and growth rates have been corrected for the unloaded volume. The total crack surface area per unit volume is found by summation of the four contributions:

$$S_V = S_{V_1} + S_{V_2} + S_{V_3} + S_{V_4} \tag{11}$$

One sees that S_V is a function of the stress-wave parameters σ_c, σ_t, t, as well as material parameters N_i, N_v^c, N_v^{sc}, $\dot{N}_v'$, $\dot{N}_v^{sc}$, K_{IC}, α. By independent experiments it is possible to establish these parameters which can, when inserted into Eq. 11, predict the fragmentation parameter S_V. There are many simplifying assumptions in the model, but it is thought that it incorporates the principal events in plane stress wave induced damage.

From S_V it is possible to calculate a mean fragment size D, by means of the simple geometric relationship[9]:

$$D = \frac{6}{S_v} \tag{12}$$

This research was supported by CETR, New Mexico Tech and the U.S. Army Research Office.

REFERENCES

1. R. A. Graham and W. P. Brooks, J. Phys. Chem. Solids, 32 (1971) 2311.
2. T. J. Ahrens, W. H. Gust, and E. B. Royce, J. Appl. Phys. 39 (1968) 4610.
3. D. Yaziv, Ph.D. Thesis, Dayton University, Ohio (1985).
4. L. H. Leme Louro, Thesis, New Mexico Institute of Mining and Technology, New Mexico (1988).
5. M. A. Meyers and L. H. L. Louro, to be published (1989).
6. S. Suresh, J. Duffy, K. Cho, and E. R. Bopp, J. Eng. Matls. Techn., Trans. ASME, (1988).
7. D. R. Curran, D. A. Shockey, and L. Seaman, J. Appl. Phys. 44 (1973) 4025.
8. L. Seaman, D. A. Shockey, and D. R. Curran, J. Appl. Phys. 47 (1976) 4814.
9. M. A. Meyers and K. K. Chawla, "Mechanical Metallurgy", Prentice-Hall, 1984, p. 497.